Published in final edited form as:
J Immunol. 2013 April 1; 190(7): 3590–3599. doi:10.4049/jimmunol.1200860.

Activation of NLRP3 inflammasome in alveolar macrophages contributes to mechanical stretch-induced lung inflammationand injury

Jianbo Wu[*,†,1], **Zhibo Yan**[‡,§,1], **David E. Schwartz**[*], **Jingui Yu**[†], **Asrar B. Malik**[‡], and **Guochang Hu**[*,‡]

[*]Department of Anesthesiology, University of Illinois College of Medicine, Chicago, IL 60612

[†]Department of Anesthesiology, Qilu Hospital of Shandong University, Jinan, 250012, China

[‡]Department of Pharmacology, University of Illinois College of Medicine, Chicago, IL 60612

[§]Department of General Surgery, Qilu Hospital of Shandong University, Jinan, 250012, China

Abstract

Mechanical ventilation of lungs is capable of activating the innate immune system and inducing sterile inflammatory response. The proinflammatory cytokine IL-1β is among the definitive markers for accurately identifying ventilator-induced lung inflammation. However, mechanisms of IL-1β release during mechanical ventilation are unknown. Here we show that cyclic stretch activates the NLRP3 inflammasomes and induces the release of IL-1β in mouse alveolar macrophages via caspase-1- and TLR4-dependent mechanisms. We also observed that NADPH oxidase subunit gp91^{phox} was dispensable for stretch-induced cytokine production whereas mitochondrial generation of reactive oxygen species was required for stretch-induced NLRP3 inflammasome activation and IL-1β release. Further, mechanical ventilation activated the NLRP3 inflammasomes in mouse alveolar macrophages and increased the production of IL-1β *in vivo*. IL-1β neutralization significantly reduced mechanical ventilation-induced inflammatory lung injury. These findings suggest that the alveolar macrophage NLRP3 inflammasome may sense lung alveolar stretch to induce the release of IL-1β, and hence may contribute to the mechanism of lung inflammatory injuryduring mechanical ventilation.

Keywords

interleukin-1β; mitochondria; reactive oxygen species; ventilator-induced lung injury

Introduction

Mechanical ventilation is necessary to support patients with acute lung injury (ALI) or its most severe form, acute respiratory distress syndrome (ARDS); however, it has also been shown to exacerbate lung injury, the so-called ventilator-induced lung injury (VILI) (1). VILI is characterized by inflammation associated with robust release of proinflammatory cytokines and activation of inflammatory signaling pathways (1). A variety of inflammatory

Correspondence and requests for reprints should be addressed to: Guochang Hu, M.D., Ph.D., Department of Pharmacology (m/c 868), University of Illinois College of Medicine, 835 South Wolcott Avenue, Chicago, Illinois 60612, USA,. Phone: (312) 996-4692, Fax: (312) 996-1225, gchu@uic.edu.

[1]Jianbo Wu and Zhibo Yan equally contributed to this work.

Disclosures

The authors have no financial conflict of interest.

mediators are released into the distal air spaces during ALI (2), and among these is IL-1β, a potent pro-inflammatory cytokine initiating and amplifying lung inflammation in patients (3). IL-1β can stimulate the production of a variety of chemokines (e.g., IL-8, MCP-1, and MIP-1α) (4). A recent study indicates that IL-1β is critical for the pathogenesis of VILI (5). Activation of the inflammatory response, including increased IL-1 signaling, is a major mechanism of alveolar barrier dysfunction in VILI (5). Studies in patients have demonstrated that IL-1β is amongst the best markers of ventilator-induced lung inflammation (6). Findings also suggest that IL-1 is a key regulator of inflammation. IL-1β receptor antagonist and anti-IL-1β antibody have been demonstrated to prevent ALI (2, 5, 7).

Alveolar macrophages (AMs) residing in the alveolar space account for 5% of peripheral lung cells (8). Under physiological condition, leukocyte population in the alveolar space is dominated by AM (comprising > 90% of the total cells) with the remainder being mainly dendritic cells and T cells. The lung parenchyma also contains macrophages (9). AMs have a central role in the maintenance of immunological homeostasis and in host-defense. In response to inflammatory stimuli, AMs are the primary source of cytokines in lungs. AMs can be rapidly activated by mechanical ventilation and thus may play an important role in the pathogenesis of VILI (10, 11). Depletion of AMs improved alveolar barrier dysfunction and lung inflammatory injury caused by high tidal volume ventilation (5, 11).

The inflammasome mainly consists of nucleotide-binding oligomerization domain-like receptor (NLR) family members containing pyrin domain (NLRP), the adaptor molecule apoptosis-associated speck-like protein containing a CARD (ASC) domain, and caspase-1 (12–14). To date, four distinct inflammasome complexes including NLRP1 (NALP1), NLRP3 (NALP3), and IPAF (NLRC4, IL-1 converting enzyme) protease-activating factor, and absent in melanoma 2 (AIM2), have been characterized (2). Among these inflammasome prototypes, NLRP3 is involved in sensing endogenous danger signals, including uric acid crystals and amyloid-β protein (15). In response to danger signals, NLRP3 interacts with pro-caspase-1 through ASC, which leads to activation of caspase-1. Active caspase-1 promotes cleavage and, therefore, maturation of proinflammatory cytokines (Pro-IL-1β, Pro–IL-18, and IL-33) (15, 16). The production of mature IL-1β is however tightly regulated. In macrophages, two signals are needed for the release of biologically active IL-1β. First, transcription of the IL-1β gene and production of cytosolic Pro-IL-1β are dependent on activation of NF-κB via, for example, TLRs. The second signal leads to cleavage of Pro-IL-1β by caspase-1 and release of the mature IL-1β (12–14).

In this study, we addressed the role of lung mechanical stretch in mediating the release of mature IL-1β via activation of the NLRP3 inflammasomes in AMs. We observed that lung cyclic stretch-induced IL-1β release was mediated by mitochondrial reactive oxygen species (ROS). Our findings collectively provide a new insight into the role of NLRP3 inflammasomes in the pathophysiology of VILI, and suggest that NLRP3 is a potential therapeutic target for dampening AM activation and thereby preventing VILI.

Materials and Methods

Mice

Male C57BL/6J, *tlr4*$^{-/-}$, and *gp91*$^{phox-/-}$ mice were purchased from the Jackson Laboratory (Bar Harbor, ME). All mice used for this study were male, 8–12 weeks of age, and weighed 25 to 30 g. Animal studies were approved by the University of Illinois Institutional Animal Care and Use Committee.

Isolation of alveolar macrophages

AMs were isolated by bronchoalveolar lavage (BAL) as described previously (17). Briefly, mice were anesthetized by intraperitoneal injection of 3 mg/kg xylazine and 75 mg/kg ketamine and then sacrificed by cardiac exsanguination. The lungs and trachea were then excised en bloc, washed in HBSS, and lavaged more than 10 times with light massaging by slowly instilling and withdrawing 1ml of warm (37°C) Ca^{2+}/Mg^{2+}-free HBSS (pH 7.4) containing EDTA (0.6 mM). BAL fluid was collected and then centrifuged at 400 g for 10 min at 4°C. The cells were then incubated in 100-mm sterilized polystyrene Petri dishes for 2 h at 37°C. The cells adhering to the bottom of dish were collected and replated for further experimental use. The purity of isolated AM was >95% as determined using fluorescently labeled antibodies (mAbs) that specifically recognize proteins expressed by mice macrophages (surface antigens F4/80 and CD11b). The viability was >98% as evaluated by trypan blue exclusion.

Cell culture

The mouse AMs were cultured at a density of 1×10^5 cells/cm^2 on collagen IV-coated dishes in DMEM containing 10% FBS without antibiotics and incubated at 37°C in an atmosphere of 5% CO_2. Confluent monolayers formed on culture dishes or BioFlex plates with elastomer membranes within 24–48 h. AM monolayers were serum-deprived for 2 h prior to experiments.

Treatment ofAMs

AMs were treated with mitochondria-targeted antioxidant SS-31 (D-Arg-2′,6′-dimethyltyrosine-Lys-Phe-NH_2, 5 μM) for 24 h, mitochondrial complex I inhibitor rotenone (10 μM) for 6h, or allopurinol (1 mM) for 6h before cyclic stretch. AMs were exposed to a caspase-1 inhibitor *N*-benzyloxycarbonyl-Tyr-Val-Ala-Asp-fluoromethyl ketone (Z-YVAD-FMK) for 1 h prior to cyclic stretch.

Crystal preparation

Monosodium urate (MSU) crystals were prepared by recrystallization from uric acid, as described previously (18). Briefly, MSU crystals were obtained by dissolving 1.68 mg of powder in 0.01 M NaOH preheated to 70°C (pH 7.1–7.2). The solution was slowly and continuously agitated at room temperature until crystals formed. The crystals were washed twice with 100% ethanol, dried, autoclaved and weighed under sterile condition. Immediately prior to experiments, the crystals were resuspended in PBS by sonication and examined under phase microscopy.

Cyclic stretching studies

AM monolayers on flexible membranes were exposed to cyclic stretch using FX-4000T Flexercell Tension Plus system (Flexcell International, McKeesport, PA) equipped with a 25-mm BioFlex loading station as previously described (19). Briefly, AM cells were seeded at standard densities (1×10^5 cells/well) onto collagen IV-coated flexible bottom BioFlex plates. After 48 h of culture, the medium was changed in each plate, and experimental plates with cell monolayers were mounted onto the Flexercell system. Based on our previous work (19), we used a pattern of cyclic stretch at a frequency of 30 cycles/min (0.5 Hz), with a stretch/relaxation relation of 1:1. Cyclic stretch was conducted at 8%, 15% and 20% changes in basement membrane surface area applied in a cyclic manner. These surface area changes correspond to 50%, 64% and 80% of total lung capacity, respectively (19, 20). Cells were stretched for 1, 2 and 4 h at 37°C in a humidified incubator containing 5% CO_2. The flexible cell-covered elastomer membranes were stretched by applying an oscillating vacuum to the underside of the 6 membranes. A computer controlled the duration, amplitude, and

frequency of the applied stretch. Non-stretched cells (static cells) were used as controls. Comparisons were made between stretched cells and control cells cultured on the same plates in the absence of cyclic strain.

Transfection of siRNA

Smart pool NLRP3, caspase-1, IPAF and AIM2 siRNAs (Dharmacon) were added to 50–70% confluent AMs in DMEM+10% FBS according to the manufacturer's protocol. Successful depletion of each respective protein was confirmed by Western blot analysis. All experiments were performed 48 h after transfection.

Measurement of IL-1β concentration

IL-1β in cell-culture media and BAL fluid was measured by using ELISA kit (R&D Systems) following the manufacturer's instructions (21).

Measurement of uric acid in cell culture supernatant

The concentration of uric acid was determined in cell culture supernatant using an Amplex Red Uric Acid/Uricase Assay Kit (Molecular Probes, Eugene, OR) according to the manufacturer's instructions. Uricase catalyzes the conversion of uric acid to allantoin, H_2O_2, and CO_2. In the presence of horseradish peroxidase, H_2O_2 reacts stochiometrically with Amplex Red reagent to generate the red-fluorescent oxidation product, resorufin, which is measured spectrophotometrically.

Determination of cell viability

Cell viability following cyclic stretch was evaluated by measurement of lactate dehydrogenase (LDH) activity in cell culture supernatants (22). LDH activity was determined by spectrophotometric analysis using the Cytotoxicity Detection Kit^{PLUS} (LDH, Roche) according to the manufacturer's protocol. Cellular LDH activity was measured after lysis of the cells with 1% Triton X-100 in PBS. The released LDH activity was expressed as a percentage of total cellular LDH activity.

Flow cytometric analysis

Mitochondria-associated ROS levels were measured in AMs by staining cells with MitoSOX (23, 24). Briefly, cells were incubated for 30 min at 37°C in a 10 μM MitoSOX™ Red (Invitrogen-Molecular Probes) solution prepared in 4:1 (v/v) DMEM/PBS. Cells were then rinsed three times with PBS, harvested with 500 μl of trypsin-EDTA solution, centrifuged at 2300 g for 5 min, and resuspended in 3 ml of fresh 2% (v/v) FBS/PBS. Stained cells were determined with a FACSCanto II flow cytometer (BD Biosciences) and data analyzed with FlowJo analytical software (TreeStar). Signals from 1×10^4 cells were acquired for each sample. The mean fluorescence of the cell sample was then normalized to the unstained control group.

Western blotting and immunoprecipitation

Western blot analysis was carried out on both the cultured medium and the cell lysates. The cell culture media were collected and concentrated by filter centrifugation (Millipore Amicon; cut-off ≤ 10,000 nominal m.w. limit). The collected medium samples were then concentrated using a commercial precipitation kit (2D Clean-up Kit; GE Healthcare). The cells were washed and lysed in a lysis buffer. Protein concentrations of the samples were determined using the bicinchoninic acid (BCA) protein assay kit (Pierce, Rockford, IL). Protein samples of concentrated medium or cell lysate supernatants were mixed with an appropriate volume of SDS sampling buffer and separated by SDS-PAGE gel (10–12%). The protein bands were then transferred onto nitrocellulose membranes by electroblotting.

The membranes were incubated with primary Abs overnight, washed and then incubated with goat anti-rabbit or anti-mouse IgG conjugated to horseradish peroxidase (1:5,000~8,000) for 60 min. Protein bands were detected using the ECL SuperSignal reagent (Pierce, Rockford, IL). Relative band densities of the various proteins were measured from scanned films using NIH ImageJ Software.

Immunoprecipitation analysis was performed as described previously (21). Macrophages were lysed in buffer containing 50 mM Tris-HCl (pH 8.0), 150 mM NaCl, 1 mM EDTA, 1% Triton X-100, 20 mM NaF, 1 mM PMSF, 1 mM Na_3VO_4, and protease inhibitor mixture. Samples were precleared using 1 mg control IgG together with protein A/G PLUS-agarose beads, and then incubated overnight at 4°C with anti-NLRP3, anti-ASC, or anti-caspase-1 Ab, followed by addition of 25 ml protein A/G PLUS-agarose beads. The resulting immunoprecipitates were dissolved in SDS-PAGE sample buffer for electrophoresis and immunoblot analysis.

Depletion of AMs in mice

Clodronate liposomes were prepared as previously described (11). Briefly, phosphatidylserine, phosphatidylcholine, and cholesterol were mixed at a molar ratio of 1:6:4 in chloroform. The chloroform is removed by rotary evaporation (100 rpm) at 40°C. A clodronate stock solution or PBS was added, and the mixture was placed under nitrogen and sonicated for 3 min. The liposome suspension was filtered through 200-nm filters. The clodronate liposome solution was then delivered to anesthetized (ketamine 90 mg/kg, i.p.) mice by nebulization.

In vivo experimental protocols

A well-established *in vivo* mouse model of VILI was utilized as described previously (25, 26). Briefly, wild type C57BL/6J and *gp91*$^{phox-/-}$ mice were anesthetized with ketamine (75 mg/kg), underwent tracheotomy and ventilated with 1% isoflurane in room air to maintain anesthesia. For high tidal volume ventilation, mice were connected to a Harvard Apparatus ventilator (MiniVent, Harvard Biosciences; Holliston, MA), with a tidal volume of 28 ml/kg, a respiratory rate of 60 breath/min, and 0 cm H_2O end-expiratory pressure. For normal volume ventilation, mice received 7 ml/kg of tidal volume, a respiratory rate of 120 breath/min and 0 cm H_2O end expiratory pressure. In order to maintain $PaCO_2$ between 35 and 45 torr (4.7–6.0 kPa), ~5 ml of dead space was added to the ventilator circuit. In some experiments, animals were pretreated with a mitochondrial ROS inhibitor SS-31 for 24 h. After mechanical ventilation, various measurements were obtained. In IL-1β neutralization experiment, at 10 min before ventilation, mice were intratracheally instilled with 100 μg anti–IL-1β or IgG isotype control (27) and then ventilated at 28 ml/kg for 2 h.

Lung tissue myeloperoxidase (MPO) assay

MPO activity, a marker for polymorphonuclear neutrophil (PMN) infiltration into the lung, was determined using a MPO assay kit (Abcam) according to manufacturer's protocol. MPO activity was expressed as change in absorbance per mg of protein (25, 26).

Determination of PMN counts in BAL fluid

At the end of experiments, BAL was performed by intratracheal injection of 1 ml of PBS followed by gentle aspiration. The lavage was repeated three times. The pooled BAL fluid was centrifuged and cell pellets were suspended in PBS. Cell suspensions were cytospun onto slides with a cytocentrifuge (Shandon, Southern Sewickley, PA). Slides were stained with Diff-Quick dye(Dade Behring, Newark, DE) and examined at a magnification of ×20

and ×40 by light microscopy. The percentage of PMNs was determined after counting 300 cells in randomly selected fields.

Assessment of pulmonary vascular permeability and edema formation in mice

Protein concentration in BAL was determined with BCA method as an index of increased permeability of the alveolar-capillary barriers (25, 26). Extravascular lung water was used as an index of lung water content and edema (26).

Reagents

Peptide SS31 was purchased from AnaSpec. Collogen IV, mitochondrial complex I inhibitor rotenone, and allopurinol were from Sigma-Aldrich. Abs for immunoblotting included NLRP3, ASC, caspas-1, Pro-IL-1β, IL-1β p17, Pro-IL-18 and IL-18 were from Santa Cruz Biotechnology. Z-YVAD-FMK was purchased from Axxora. Anti-IL-1β (B122) Ab and Armenian hamster IgG isotype control (HTK888) were obtained from BioLegend (San Diego, CA).

Statistical analysis

Data are expressed as mean ± SD. One-way ANOVA and Student's Newman-Keuls test for post hoc comparisons were used to determine differences between control and experimental groups. Student *t* test was performed for paired samples. Parameter changes between different groups over time were evaluated by a two-way ANOVA with repeated measures. Statistical analyses were performed using SPSS 15.0 statistics software. A value of $p < 0.05$ was considered statistically significant.

Results

Cyclic stretch induces the release of IL-1β and IL-18 by mouse AMs

To test the hypothesis that inflammasomes sense mechanical stretch in AMs, we first determined the effects of cyclic stretch on IL-1β and IL-18 production, known to depend on inflammasome activation (12, 28). Western blot analysis showed that cyclic stretch induced magnitude- and time-dependent proteolytic cleavage of Pro-IL-1β and Pro-IL-18, and resulted in the release of mature 17-kDa IL-1β and 18-kDa IL-18 in media supernatants (Fig. 1*A* and 1*B*, Supplemental Fig. 1*A*–1*D*). The appearance of IL-1β in the cell culture medium was verified by ELISA assay (Fig. 1*C* and 1*D*). Consistent with previous observations (29, 30), 17-kDa IL-1β and 18-kDa IL-18 were undetected intracellularly (data not shown). Cyclic stretch had no effect on protein expression of Pro-IL-1β and Pro-IL-18. Processing and release of IL-1β has been shown to occur with significant cell death and cell lysis (31, 32). Thus, we also determined the effects of cyclic stretch on cell viability (LDH release). As shown in Fig. 1*E*, cyclic stretch used in our study did not alter LDH release. Together, these data suggest that cyclic stretch alone is able to induce mature IL-1β and IL-18 production in murine AMs.

Cyclic stretch-induced release of IL-1β is caspase-1-dependent

Inflammasome activation resulted in recruitment and activation of caspase-1, the key regulatory component of the inflammasome multiprotein complex responsible for processing of Pro-IL-1β into the mature IL-1β (18, 33). Since caspase-1 is secreted after inflammasome activation, we analyzed cell lysate from cyclic stretch-stimulated macrophages for the presence of mature caspase-1 using immunoblotting. As shown in Fig. 2*A* and Supplemental Fig. 1*E*, active caspase-1 was not detected in control (static) cells. However, we observed the appearance of the p10 product of caspase-1 following cyclic stretch. Consistent with changes in IL-1β release, cyclic stretch also induced magnitude- and time-dependent

proteolytic cleavage of pro–caspase-1 and caspase-1 production (Fig. 2*A* and 2*B*, Supplemental Fig. 1*E* and 1*F*), indicating that mechanical stretch induced proteolytic processing of caspase-1. We next evaluated the role of caspase-1 in mechanical stretch-induced IL-1β release using a caspase-1 specific inhibitor, Z-YVAD-FMK. As shown in Fig. 2*C* and Supplemental Fig. 1*G*, Z-YVAD-FMK in a dose-dependent manner abolished mechanical stretch-induced increase in IL-1β release. The similar effect of Z-YVAD-FMK on mature IL-1β in the cell culture medium following stretch was verified by ELISA assay (Fig. 2*D*). Furthermore, depletion of pro-caspase-1 with a specific siRNA abolished stretch-induced IL-1β release (Fig. 2*E*, 2*F*, Supplemental Fig. 1*H*). These data suggest that maturation of IL-1β induced by cyclic stretch was mediated via caspase-1 pathway.

Cyclic stretch activates NLRP3 inflammasome pathway

The assembly of the NLRP3 inflammasome complex is an initial step of inflammasome activation requiring a pyrin domain (PYD)/PYD interaction between ASC and NLRP3 and caspase recruitment domain/caspase recruitment domain interaction between ASC and pro-caspase-1 for caspase-1 activation, and subsequent IL-1β release (14). We observed that the association of the complex consisting of NLRP3, ASC and caspase-1 in AMs was induced at 1 h after cyclic stretch and further increased between 2 and 4 h (Fig. 3*A*, Supplemental Fig. 2*A*), suggesting the ability of mechanical stretch to activate NLRP3 inflammasome.

To further assess the contribution of NLRP3 to IL-1β and IL-18 release induced by cyclic stretch in AMs, we knocked down NLRP3 with a specific siRNA. Treatment of AMs with NLRP3-targeted siRNA diminished NLRP3 protein level by 80% (Fig. 3*B*). We found that NLRP3 knockdown abolished the effect of cyclic stretch on activation of capase-1 and subsequent release of mature IL-1β (Fig. 3*B*, 3*C*, Supplemental Fig. 2*B*) and IL-18 (Fig. 3*B*, Supplemental Fig. 2*C*), with no effect on protein expression of pro-caspase-1, Pro-IL-1β and Pro-IL-18. In cooperation with NLRP3 and IPAF, AIM2 has been shown to play an important role in activation of caspase-1 during bacterial infection (34). However, in contrast to NLRP3 inflammasome, we observed that siRNA-induced depletion of IPAF and AIM2 had no effect on cyclic stretch-induced capase-1 activation and subsequent release of mature IL-1β and IL-18 (Fig. 3*B* and 3*C*, Supplemental Fig. 2*B* and 2*C*), indicating that activation of caspase-1 and the release of IL-1β and IL-18 by mechanical stretch were mediated byNLRP3 inflammasome but not by IPAF and AIM2 inflammasomes.

Mitochondria ROS are required for inflammasome activation induced by cyclic stretch

Since mitochondrial ROS production was found to be important in NLRP3 inflammasome activation (15), we determined whether mitochondrial ROS were generated in response to cyclic stretch. As shown in Fig. 4*A*, exposure of AMs to cyclic stretch significantly increased mitochondrial ROS fluorescence. Treatment of macrophages with the mitochondria-targeted antioxidant SS-31, a scavenger for mitochondrial ROS (35), reduced the levels of mitochondrial ROS (Fig. 4*A* and 4*B*). SS-31 in a dose-dependent manner also inhibited cyclic stretch-induced caspase-1 activation and IL-1β production (Fig. 4*C*, 4*D*, Supplemental Fig. 2*D*). Treatment with the mitochondrial complex I inhibitor rotenone known to result in ROS generation (23, 36), enhanced caspase-1 activation (Fig. 4*E*) and IL-1β release (Fig. 4*E*, 4*F*, Supplemental Fig. 2*E*) caused by cyclic stretch in AMs. These data together demonstrate that mitochondrial ROS may be required for the IL-1β release in AMs induced by mechanical stretch.

NADPH-derived ROS were shown to be essential for fatty acid-induced inflammasome activation (28). To determine whether NADPH-derived ROS are involved in NLRP3 inflammasome activation and IL-1β release following cyclic stretch, we isolated AMs from *gp91*$^{phox-/-}$ mice. Deletion of gp91^{phox} did not inhibit stretch-induced caspase-1 activation

and IL-1β release (Fig. 5*A*, 5*B*, Supplemental Fig. 3*A*). Further analysis using flow cytometry showed that $gp91^{phox}$ deletion did not alter mitochondrial ROS production induced by stretch (Fig. 5*C* and 5*D*). These results therefore exclude a role for NADPH oxidase-derived ROS in NLRP3 inflammasome activation in AMs. Taken together, mechanical stretch activates NLRP3 inflammasome via mitochondrial ROS dependent signaling pathway.

Uric acid released from AMs following cyclic stretch activates NLRP3 inflammasome partially through mitochondrial ROS

Uric acid is present in normal cells and released from dying cells (37). Uric acid crystallizes at concentrations exceeding limits of solubility (~6.8 mg/dL or even lower under conditions of reduced pH or temperature) and it is capable of activating the NLRP3 inflammasome following crystallization (18). We observed that uric acid concentration in the medium after stretch was significantly increased (7.8 μg/ml vs. 0.2 μg/ml) (Fig. 6*A*). Allopurinol, the inhibitor of uric acid synthesis, dose-dependently decreased uric acid levels, with complete inhibition of uric acid production occurring at 10 mM (Fig. 6*A*). This concentration of allopurinol was not cytotoxic (data not shown). Accordingly, 10 mM of allopurinol was chosen and used in the subsequent experiments. Exposure of AMs to allopurinol attenuated, but did not abolish cyclic stretch-induced caspase-1 activation and IL-1β production (Fig. 6*B*, Supplemental Fig. 3*B*). Allopurinol had no effects on the release of IL-1β in non-stretched AMs and synthesis of Pro-IL-1β (Fig. 6*B*, Supplemental Fig. 3*B*). To determine whether uric acid-induced IL-1β production following stretch was dependent on mitochondrial ROS, we investigated the role of uric acid in mitochondrial ROS generation. Exogenous MSU in a dose-dependent manner (2.5 ~ 10 μg/ml) stimulated mitochondrial ROS generation (Fig. 6*C* and 6*D*) and IL-1β release (Fig. 6*E*). Allopurinol did not completely inhibit mitochondrial ROS generation (Fig. 6*F*), suggesting that mitochondrial ROS production following cyclic stretch was partially dependent on uric acid.

Cyclic stretch-induced release of IL-1β is dependent of TLR4 signaling

Pro-IL-1β biosynthesis and intracellular accumulation depend upon TLR4 signaling activation of NF-κB. To determine whether cyclic stretch-induced inflammasome activation is TLR4 dependent, we mechanically stretched AMs isolated from $tlr4^{-/-}$mice. Compared to wild type AMs, $tlr4^{-/-}$AMs exhibited a dramatic decrease in the protein levels of Pro-IL-1β. Although cyclic stretch caused a slight increase in IL-1β release in $tlr4^{-/-}$AMs, the concentration of IL-1β following stretch in the medium was much less than that in wild type AMs (Fig. 7*A*, Supplemental Fig. 3*C*, and Fig. 7*B*). Flow cytometric data showed that increased mitochondrial ROS following cyclic stretch in wild type AMs were not affected in $tlr4^{-/-}$AMs (Fig. 7*C* and 7*D*). These results suggest that cyclic stretch-induced IL-1β release depends on TLR4 signaling-mediated Pro-IL-1β generation.

High tidal volume mechanical ventilation activates NLRP3 inflammasome

To address whether mechanical stretch could activate NLRP3 inflammasome in lungs, we used a well-established mouse model of VILI (25, 26). The assembly of NLRP3, ASC and caspase-1 in lungs ventilated with high tidal volume was induced at 1 h after mechanical ventilation and further increased within 4 h. Caspase-1 cleavage as well as mature IL-1β and IL-18 were detected at 1 h and further increased within 4 h (Fig. 8*A*). The IL-1β concentration in BAL fluid, representing IL-1β released from pulmonary cells, was elevated at 1 h after mechanical ventilation (Fig. 8*B*). Mechanical ventilation-induced NLRP3 inflammasome activation (Fig. 8*A*), release of IL-1β (Fig. 8*A*, Supplemental Fig. 4*A*, and Fig. 8*B*) and IL-18 (Fig. 8*A* and Supplemental Fig. 4*B*) were significantly attenuated by pretreatment of mice with a mitochondrial ROS inhibitor, but not by depletion of NADPH oxidase-derived ROS.

To determine the contribution of AMs to IL-1β release in the lung, AMs were depleted using a liposomal clodronate technique (11). Lavageable AM count was reduced by 75% at 4 days with a 10-ml aerosolized dose of 20 mg/ml clodronate liposome solution. Depletion of AMs resulted in significantly reduced NLRP3 inflammasome activation (Fig. 8*C*) and reduced release of IL-1β (Fig. 8*C*, Supplemental Fig. 4*C*, and Fig. 8*D*) and IL-18 (Fig. 8*C* and Supplemental Fig. 4*D*) attributable to mechanical ventilation. These findings suggest that high tidal mechanical ventilation activates pulmonary NLRP3 inflammasomes and that AMs may play a key role in mechanical stretch-induced IL-1β generation in lungs.

To determine the importance of IL-1β in mechanical ventilation-induced inflammatory lung injury, we investigated the effects of IL-1β neutralization on lung inflammation and injury caused by high tidal volume ventilation. Mechanical ventilation at high tidal volume (28 ml/kg) induced an increase in trans-alveolar protein permeability (Supplemental Fig. 4*E*) and lung edema formation (Supplemental Fig. 4*F*). These effects were significantly reduced in mice pretreated with IL-1β Ab (Supplemental Fig. 4*E* and 4*F*). Mechanical ventilation caused a marked increase in lung MPO levels (Supplemental Fig. 4*G*) and PMN counts in BAL fluid (Supplemental Fig. 4*H*). These responses were blunted in mice pretreated with IL-1β Ab (Supplemental Fig. 4*G* and 4*H*). IL-1β Ab alone had no effect on pulmonary vascular permeability, edema formation, and PMN infiltration.

Discussion

Mechanical ventilation induces the production of IL-1β in lungs of animal models (5) and patients (6). Because IL-1β is a pro-inflammatory cytokine and a mediator of sterile inflammation that acts through IL-1 receptor (38, 39), it may have a role in the mechanism of lung inflammation and injury induced by mechanical stretch. In the present study, using *in vitro* model of cyclic stretch and *in vivo* model of VILI in mice, we demonstrated the central role of mechanical stretch in activating NLRP3 inflammasome in AMs which in turn mediated IL-1β release via mitochondrial ROS-dependent signaling. These results are in accord with recent studies in $Nlrp3^{-/-}$mice, highlighting the importance of NLRP3 inflammasome in mediating lung inflammation during VILI (40). Previous studies also showed that genetic deletion of IL-18 or caspase-1 conferred resistance to VILI in mouse models (41). Our results taken in the context of previous studies provide support for the central role of NLRP3 inflammasome activation in AMs secondary to mechanical stretch in the mechanism of lung inflammation and injury.

To address the molecular basis of inflammasome activation in response to mechanical stretch, we focused on ROS generation by AMs. ROS generation has been shown to activate NLRP3 inflammasome (18, 33). Studies have suggested a role for NADPH oxidases-derived ROS in NLRP3 activation (33, 42) whereas other studies pointed to mitochondrial ROS in activating NLRP3 inflammasome in macrophage (23, 24). Macrophages lacking functional NADPH oxidase (NOX)1, NOX2 and NOX4 responded normally to NLRP3 stimulation (23). Studies employing inhibition of mitochondrial ROS and analysis of mice lacking gene for $gp91^{phox}$ subunit of NADPH oxidase demonstrated that mitochondria ROS were responsible for NLRP3 inflammasome activation and mediated inflammation induced by mechanical ventilation. Mitochondrial ROS promoted NLRP3 inflammasome complex assembly, caspase-1 activation and subsequent IL-1β release in AMs and whole lungs. The basis of mitochondrial ROS-induced NLRP3 inflammasome activation is not clear. One tenable mechanism is that mitochondrial ROS can induce translocation of NLRP3 to mitochondria-associated endoplasmic reticulum membranes, where ASC is recruited, thereby activating NLRP3 inflammasome (43). Another possibility is that mitochondrial ROS can promote mitochondrial permeability transition, which may facilitate cytosolic

release of mitochondria DNA, and stimulate activation of NLRP3 inflammasome, resulting in the production of IL-1β and IL-18 (23, 44).

The production of mitochondrial ROS in response to mechanical stretch has been shown in non-phagocytic cells including endothelial cells (45) and pulmonary epithelial cells (46). Here, we showed that mechanical stretch also stimulated mitochondrial ROS generation in AMs. Activation of mitochondrial ROS system may be the result of distention and deformation of mitochondria following stretch and alterations in mitochondrial K^+ ATP channel activity (46). Another mechanism may involve stretch-induced uric acid production which stimulates mitochondrial ROS generation by as yet an unidentified mechanism.

Uric acid, a product of purine catabolism, is released from damaged cells in response to variety of stresses. At a high concentration, uric acid precipitates and forms crystals that are internalized, resulting in activation of NLRP3 inflammasome (18, 38, 47). The mechanism by which endocytosed uric acid crystals are sensed by the NLRP3 inflammasome is currently not known and neither is it clear whether crystals directly interact with NLRP3 or whether sensing occurs via intermediary proteins (18). Our data however showed that cyclic stretch induced uric acid release from AMs. Since in our model, inhibition of mitochondrial ROS completely abolished IL-1β release following mechanical stretch, it appears that uric acid may be released upon stretch, contributing to activation of NLRP3 inflammasome through enhancement of mitochondrial ROS production. Taken together, these findings show that stretch-induced uric acid can activate NLRP3 inflammasome partially through the stimulation of mitochondrial ROS production.

In the present study, we observed that mechanical stretch induced the maturation and secretion of IL-1β and IL-18 in AMs via NLRP3 inflammasome activation. IL-1β and IL-18 are two closely related IL-1 family cytokines that function as key mediators of host immune response (48). Our results demonstrated that IL-1β neutralization significantly reduced mechanical ventilation-induced inflammatory lung injury. A recent study has shown that mechanical ventilation enhanced IL-18 levels in mouse lung and that anti-IL-18–neutralizing Ab treatment or genetic deletion of IL-18 reduced lung injury following mechanical ventilation (41). These findings together with ours suggest that both IL-1β and IL-18 participate in the pathogenesis of lung inflammation and injury associated with VILI secondary to activation of NLRP3 inflammasome.

In summary, this study for the first time to our knowledge demonstrates the essential role of NLRP3 inflammasome in AMs in the pathogenesis of VILI. Mechanical stretch stimulates mitochondrial ROS production in AMs which in turn signals assembly of ASC, NLRP3 and caspase-1 to activate NLRP3 inflammasome, leading to the processing and maturation of Pro-IL-1β into the active IL-1β variant. TLR4 signaling also plays an important role in Pro-IL-1β expression and subsequent IL-1β secretion. Mechanical stretch-induced uric acid production has an additional effect, which maybe enhance mitochondrial ROS generation and thereby amplify NLRP3 inflammasome activation in response to cyclic stretch of AMs (Fig. 9). The results point to potential therapeutic approaches to targeting NLRP3 inflammasome in AMs for treatment of VILI.

Supplementary Material

Refer to Web version on PubMed Central for supplementary material.

Acknowledgments

The authors would like to thank Brenda Russell, Ph.D. (Department of Physiology and Biophysics, University of Illinois at Chicago) for access and training in the use of FX-4000T Flexercell Tension Plus system. The authors are

also indebted to Erik Swanson and Golnar Doroudian (Department of Physiology and Biophysics, University of Illinois at Chicago) for technical assistance.

This work was supported by NIH NHLBI grants HL104092 and Natural Science Foundation of China (81070058).

Abbreviations used in this paper

AIM2	absent in melanoma 2
ALI	acute lung injury
AM	alveolar macrophage
ARDS	acute respiratory distress syndrome
ASC	apoptosis-associated speck-like protein containing a CARD domain
BAL	bronchoalveolar lavage
BCA	bicinchoninic acid
LDH	lactate dehydrogenase
MPO	myeloperoxidase
MSU	monosodium urate
NLRP3	nucleotide-binding oligomerization domain-like receptor containing pyrin domain 3
NOX	NADPH oxidase
PMN	polymorphonuclear neutrophil
ROS	reactive oxygen species
siRNA	small interfering RNA
VILI	ventilator-induced lung injury

References

1. Del Sorbo L, Slutsky AS. Acute respiratory distress syndrome and multiple organ failure. Curr Opin Crit Care. 2011; 17:1–6. [PubMed: 21157315]
2. Ganter MT, Roux J, Miyazawa B, Howard M, Frank JA, Su G, Sheppard D, Violette SM, Weinreb PH, Horan GS, Matthay MA, Pittet JF. Interleukin-1β causes acute lung injury via αaβ5 and αvβ6 integrin-dependent mechanisms. Circ Res. 2008; 102:804–812. [PubMed: 18276918]
3. Dinarello CA. Biologic basis for interleukin-1 in disease. Blood. 1996; 87:2095–2147. [PubMed: 8630372]
4. Goodman RB, Pugin J, Lee JS, Matthay MA. Cytokine-mediated inflammation in acute lung injury. Cytokine Growth Factor Rev. 2003; 14:523–535. [PubMed: 14563354]
5. Frank JA, Pittet JF, Wray C, Matthay MA. Protection from experimental ventilator-induced acute lung injury by IL-1 receptor blockade. Thorax. 2008; 63:147–153. [PubMed: 17901159]
6. Conway Morris A, Kefala K, Wilkinson TS, Moncayo-Nieto OL, Dhaliwal K, Farrell L, Walsh TS, Mackenzie SJ, Swann DG, Andrews PJ, Anderson N, Govan JR, Laurenson IF, Reid H, Davidson DJ, Haslett C, Sallenave JM, Simpson AJ. Diagnostic importance of pulmonary interleukin-1β and interleukin-8 in ventilator-associated pneumonia. Thorax. 2010; 65:201–207. [PubMed: 19825784]
7. Opitz B, van Laak V, Eitel J, Suttorp N. Innate immune recognition in infectious and noninfectious diseases of the lung. Am J Respir Crit Care Med. 2010; 181:1294–1309. [PubMed: 20167850]
8. Dusinska M, Kovacikova Z, Vallova B, Collins A. Responses of alveolar macrophages and epithelial type II cells to oxidative DNA damage caused by paraquat. Carcinogenesis. 1998; 19:809–812. [PubMed: 9635867]

9. Holt PG, Strickland DH, Wikstrom ME, Jahnsen FL. Regulation of immunological homeostasis in the respiratory tract. Nat Rev Immunol. 2008; 8:142–152. [PubMed: 18204469]
10. Eyal FG, Hamm CR, Parker JC. Reduction in alveolar macrophages attenuates acute ventilator induced lung injury in rats. Intensive Care Med. 2007; 33:1212–1218. [PubMed: 17468847]
11. Frank JA, Wray CM, McAuley DF, Schwendener R, Matthay MA. Alveolar macrophages contribute to alveolar barrier dysfunction in ventilator-induced lung injury. Am J Physiol. 2006; 291:L1191–1198.
12. Schroder K, Tschopp J. The inflammasomes. Cell. 2000; 140:821–832. [PubMed: 20303873]
13. Van de Veerdonk FL, Netea MG, Dinarello CA, Joosten LA. Inflammasome activation and IL-1β and IL-18 processing during infection. Trends Immunol. 2011; 32:110–116. [PubMed: 21333600]
14. Chen GY, Nunez G. Sterile inflammation: sensing and reacting to damage. Nat Rev Immunol. 2010; 10:826–837. [PubMed: 21088683]
15. Martinon F, Mayor A, Tschopp J. The inflammasomes: guardians of the body. Ann Rev Immunol. 2009; 27:229–265. [PubMed: 19302040]
16. Yu HB, Finlay BB. The caspase-1 inflammasome: a pilot of innate immune responses. Cell Host Microbe. 2008; 4:198–208. [PubMed: 18779046]
17. Lavnikova N, Prokhorova S, Helyar L, Laskin DL. Isolation and partial characterization of subpopulations of alveolar macrophages, granulocytes, and highly enriched interstitial macrophages from rat lung. Am J Respir Cell Mol Biol. 1993; 8:384–392. [PubMed: 8476632]
18. Martinon F, Petrilli V, Mayor A, Tardivel A, Tschopp J. Gout-associated uric acid crystals activate the NLRP3 inflammasome. Nature. 2006; 440:237–241. [PubMed: 16407889]
19. Wang Y, Minshall RD, Schwartz DE, Hu G. Cyclic stretch induces alveolar epithelial barrier dysfunction via calpain-mediated degradation of p120-catenin. Am J Physiol. 2011; 301:L197–206.
20. Tschumperlin DJ, Margulies SS. Alveolar epithelial surface area-volume relationship in isolated rat lungs. J Appl Physiol. 1999; 86:2026–2033. [PubMed: 10368370]
21. Wang YL, Malik AB, Sun Y, Hu S, Reynolds AB, Minshall RD, Hu G. Innate immune function of the adherens junction protein p120-catenin in endothelial response to endotoxin. J Immunol. 2011; 186:3180–3187. [PubMed: 21278343]
22. Dehne N, Kerkweg U, Otto T, Fandrey J. The HIF-1 response to simulated ischemia in mouse skeletal muscle cells neither enhances glycolysis nor prevents myotube cell death. Am J Physiol. 2007; 293:R1693–1701.
23. Zhou R, Yazdi AS, Menu P, Tschopp J. A role for mitochondria in NLRP3 inflammasome activation. Nature. 2011; 469:221–225. [PubMed: 21124315]
24. Nakahira K, Haspel JA, Rathinam VA, Lee SJ, Dolinay T, Lam HC, Englert JA, Rabinovitch M, Cernadas M, Kim HP, Fitzgerald KA, Ryter SW, Choi AM. Autophagy proteins regulate innate immune responses by inhibiting the release of mitochondrial DNA mediated by the NLRP3 inflammasome. Nat Immunol. 2011; 12:222–230. [PubMed: 21151103]
25. Hu G, Malik AB, Minshall RD. Toll-like receptor 4 mediates neutrophil sequestration and lung injury induced by endotoxin and hyperinflation. Crit Care Med. 2010; 38:194–201. [PubMed: 19789446]
26. Liu D, Yan Z, Minshall RD, Schwartz DE, Chen Y, Hu G. Activation of calpains mediates early lung neutrophilic inflammation in ventilator-induced lung injury. Am J Physiol Lung Cell Mol Physiol. 2012; 302:L370–379. [PubMed: 22140070]
27. Provoost S, Maes T, Pauwels NS, Vanden Berghe T, Vandenabeele P, Lambrecht BN, Joos GF, Tournoy KG. NLRP3/caspase-1-independent IL-1beta production mediates diesel exhaust particle-induced pulmonary inflammation. J Immunol. 2011; 187:3331–3337. [PubMed: 21844393]
28. Wen H, Gris D, Lei Y, Jha S, Zhang L, Huang MT, Brickey WJ, Ting JP. Fatty acid-induced NLRP3-ASC inflammasome activation interferes with insulin signaling. Nat Immunol. 2011; 12:408–415. [PubMed: 21478880]
29. Carta S, Tassi S, Pettinati I, Delfino L, Dinarello CA, Rubartelli A. The rate of interleukin-1beta release in different myeloid cells varies with the extent of redox response to Toll-like receptor triggering. J Biol Chem. 2011; 286:27069–27080. [PubMed: 21628463]

30. Rubartelli A, Cozzolino F, Talio M, Sitia R. A novel secretory pathway for interleukin-1 beta, a protein lacking a signal sequence. EMBO J. 1990; 9:1503–1510. [PubMed: 2328723]
31. Le Feuvre RA, Brough D, Iwakura YK, Rothwell Takeda NJ. Priming of macrophages with lipopolysaccharide potentiates P2X7-mediated cell death via a caspase-1-dependent mechanism, independently of cytokine production. J Biol Chem. 2002; 277:3210–3218. [PubMed: 11706016]
32. Hogquist KA, Unanue ER, Chaplin DD. Release of IL-1 from mononuclear phagocytes. J Immunol. 1991; 147:2181–2186. [PubMed: 1918954]
33. Dostert C, Petrilli V, Van Bruggen R, Steele C, Mossman BT, Tschopp J. Innate immune activation through NLRP3 inflammasome sensing of asbestos and silica. Science. 2008; 320:674–677. [PubMed: 18403674]
34. Tsuchiya K, Hara H, Kawamura I, Nomura T, Yamamoto T, Daim S, Dewamitta SR, Shen Y, Fang R, Mitsuyama M. Involvement of absent in melanoma 2 in inflammasome activation in macrophages infected with Listeria monocytogenes. J Immunol. 2010; 185:1186–1195. [PubMed: 20566831]
35. Dai DF, Chen T, Szeto H, Nieves-Cintron M, Kutyavin V, Santana LF, Rabinovitch PS. Mitochondrial targeted antioxidant Peptide ameliorates hypertensive cardiomyopathy. J Am Coll Cardiol. 2011; 58:73–82. [PubMed: 21620606]
36. Li N, Ragheb K, Lawler G, Sturgis J, Rajwa B, Melendez JA, Robinson JP. Mitochondrial complex I inhibitor rotenone induces apoptosis through enhancing mitochondrial reactive oxygen species production. J Biol Chem. 2003; 278:8516–25. [PubMed: 12496265]
37. Shi Y, Evans JE, Rock KL. Molecular identification of a danger signal that alerts the immune system to dying cells. Nature. 2003; 425:516–521. [PubMed: 14520412]
38. Chen CJ, Kono H, Golenbock D, Reed G, Akira S, Rock KL. Identification of a key pathway required for the sterile inflammatory response triggered by dying cells. Nature Med. 2007; 13:851–856. [PubMed: 17572686]
39. Kono H, Karmarkar D, Iwakura Y, Rock KL. Identification of the cellular sensor that stimulates the inflammatory response to sterile cell death. J Immunol. 2010; 184:4470–4478. [PubMed: 20220089]
40. Kuipers MT, Aslami H, Janczy JR, van der Sluijs KF, Vlaar AP, Wolthuis EK, Choi G, Roelofs JJ, Flavell RA, Sutterwala FS, Bresser P, Leemans JC, van der Poll T, Schultz MJ, Wieland CW. Ventilator-induced lung injury is mediated by the NLRP3 inflammasome. Anesthesiology. 2012; 116:1104–1115. [PubMed: 22531249]
41. Dolinay T, Kim SY, Howrylak J, Hunninghake GM, An CH, Fredenburgh L, Massaro AF, Rogers A, Gazourian L, Nakahira K, Haspel JA, Landazury R, Eppanapally S, Christie JD, Meyer NJ, Ware LB, Christiani DC, Ryter SW, Baron RM, Choi AM. Inflammasome-regulated cytokines are critical mediators of acute lung injury. Am J Respir Crit Care Med. 2012; 185:1225–1234. [PubMed: 22461369]
42. Cruz CM, Rinna A, Forman HJ, Ventura AL, Persechini PM, Ojcius DM. ATP activates a reactive oxygen species-dependent oxidative stress response and release of proinflammatory cytokines in macrophages. J Biol Chem. 2007; 282:2871–9. [PubMed: 17132626]
43. Sorbara MT, Girardin SE. Mitochondrial ROS fuel the inflammasome. Cell Res. 2011; 21:558–560. [PubMed: 21283134]
44. Kepp O, Galluzzi L, Kroemer G. Mitochondrial control of the NLRP3 inflammasome. Nat Immunol. 2011; 12:199–200. [PubMed: 21321591]
45. Waters CM. Reactive oxygen species in mechanotransduction. Am J Physiol. 2004; 287:L484–485.
46. Chapman KE, Sinclair SE, Zhuang D, Hassid A, Desai LP, Waters CM. Cyclic mechanical strain increases reactive oxygen species production in pulmonary epithelial cells. Am J Physiol Lung Cell Mol Physiol. 2005; 289:L834–841. [PubMed: 15964900]
47. Gasse P, Riteau N, Charron S, Girre S, Fick L, Petrilli V, Tschopp J, Lagente V, Quesniaux VF, Ryffel B, Couillin I. Uric acid is a danger signal activating NLRP3 inflammasome in lung injury inflammation and fibrosis. Am J Respir Crit Care Med. 2009; 179:903–913. [PubMed: 19218193]

48. Zaki MH, Boyd KL, Vogel P, Kastan MB, Lamkanfi M, Kanneganti TD. The NLRP3 inflammasome protects against loss of epithelial integrity and mortality during experimental colitis. Immunity. 2010; 32:379–91. [PubMed: 20303296]

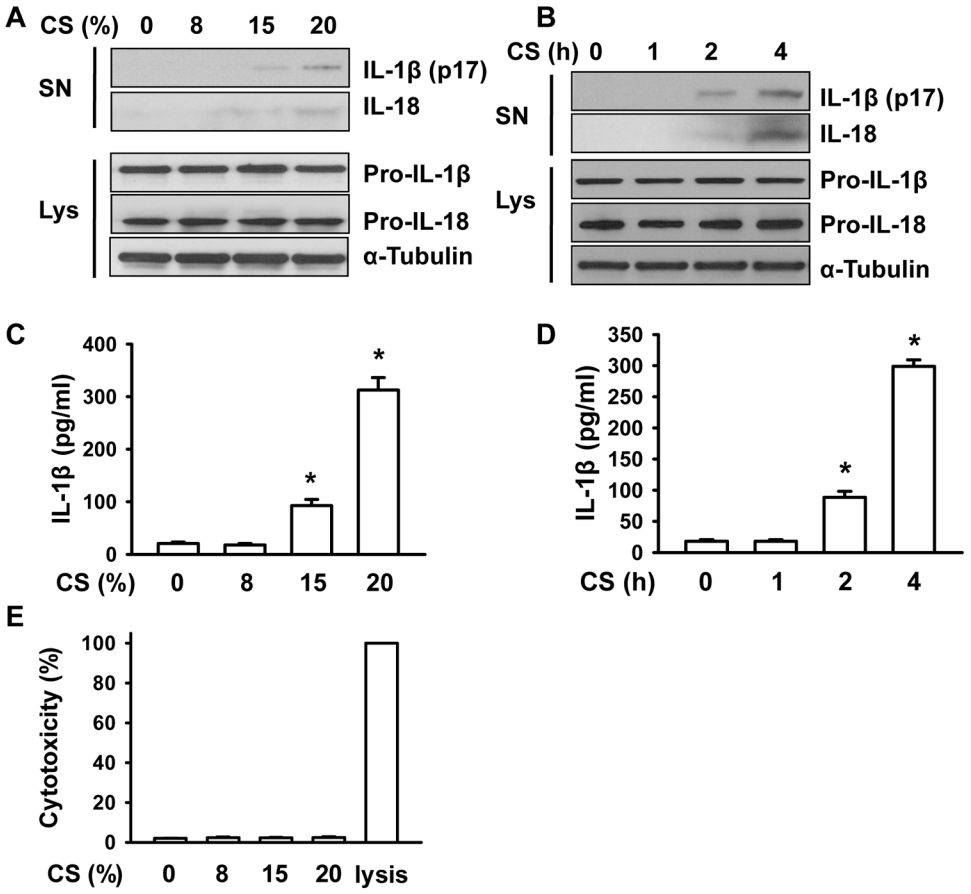

FIGURE 1. Cyclic stretch induces the release of active forms of IL-1β and IL-18 from mouse AMs

A, Mouse AMs were cyclically stretched at the levels of 0, 8, 15 and 20% for 4 h. Following cyclic stretch (CS), the release of mature IL-1β and IL-18 was measured in the culture supernatants (SN) of AMs by Western blot analysis. The levels of Pro-IL-1β and Pro-IL-18 were determined in AMs cell lysates (Lys) after cyclic stretch. ***B,*** Mouse AMs were exposed to 20% cyclic stretch for the indicated times. Following cyclic stretch (CS), the release of mature IL-1β and IL-18 was measured in the culture supernatants (SN) of AMs by Western blot analysis. The levels of Pro-IL-1β and Pro-IL-18 were determined in AMs cell lysates (Lys) after cyclic stretch. ***C***, The levels of IL-1β in the culture medium following different magnitudes of cyclic stretch were detected by ELISA. ***D***, The levels of IL-1β in the culture medium following 20% cyclic stretch for different time intervals were detected by ELISA. ***E***. Mouse AMs were cyclically stretched at the levels of 0, 8, 15 and 20% for 4 h. The concentrations of LDH were measured in supernatants to evaluate cell cytoxicity. Data are means from three independent experiments. *$p < 0.05$ vs. control group (static).

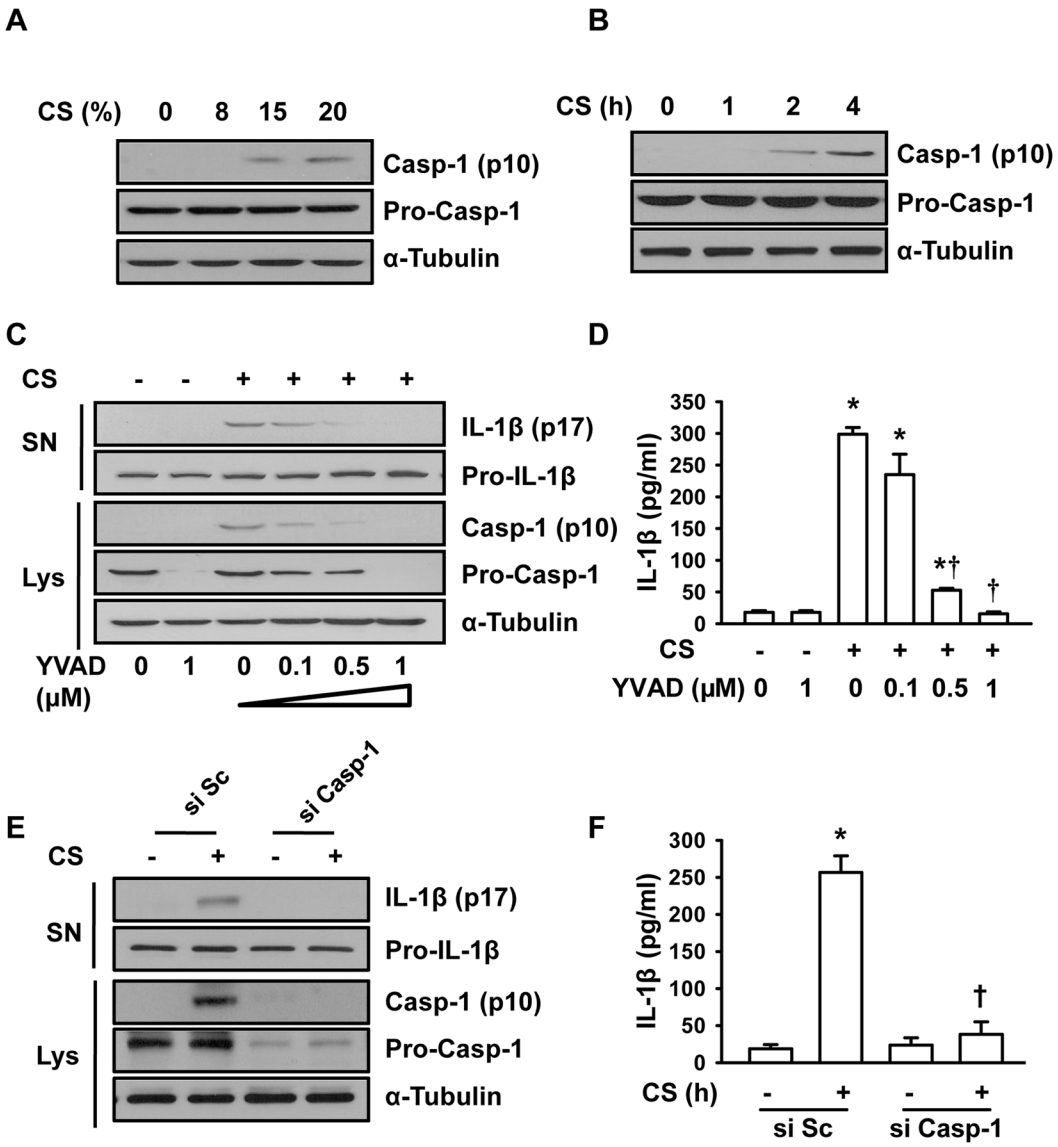

FIGURE 2. Cyclic stretch (CS)-induced IL-1β release is caspase-1-dependent

A, Mouse AMs were cyclically stretched at the levels of 0, 8, 15 and 20% for 4 h. The levels of caspase-1 (Casp-1) were detected by Western blotting. ***B***, Mouse AMs were exposed to 20% cyclic stretch for the indicated times. After stretch, the levels of caspase-1 were detected by Western blotting. ***C***, Effects of Casp-1 specific inhibitor ac-YVAD-FMK (YVAD) on IL-1β release, and expressions of Pro-IL-1β, Pro-Casp-1, and mature Casp-1. ***D***. The levels of IL-1β were detected by ELISA. ***E***. Effect of Casp-1 siRNA on IL-1β release, Pro-IL-1β, Pro-Casp-1, mature Casp-1. A scrambled siRNA (si Sc) was used as a negative control. ***F***. The levels of IL-1β were detected by ELISA. *p <0.05, vs. control group (static). Data are means from three independent experiments. † p <0.05 vs CS control group (stretched).

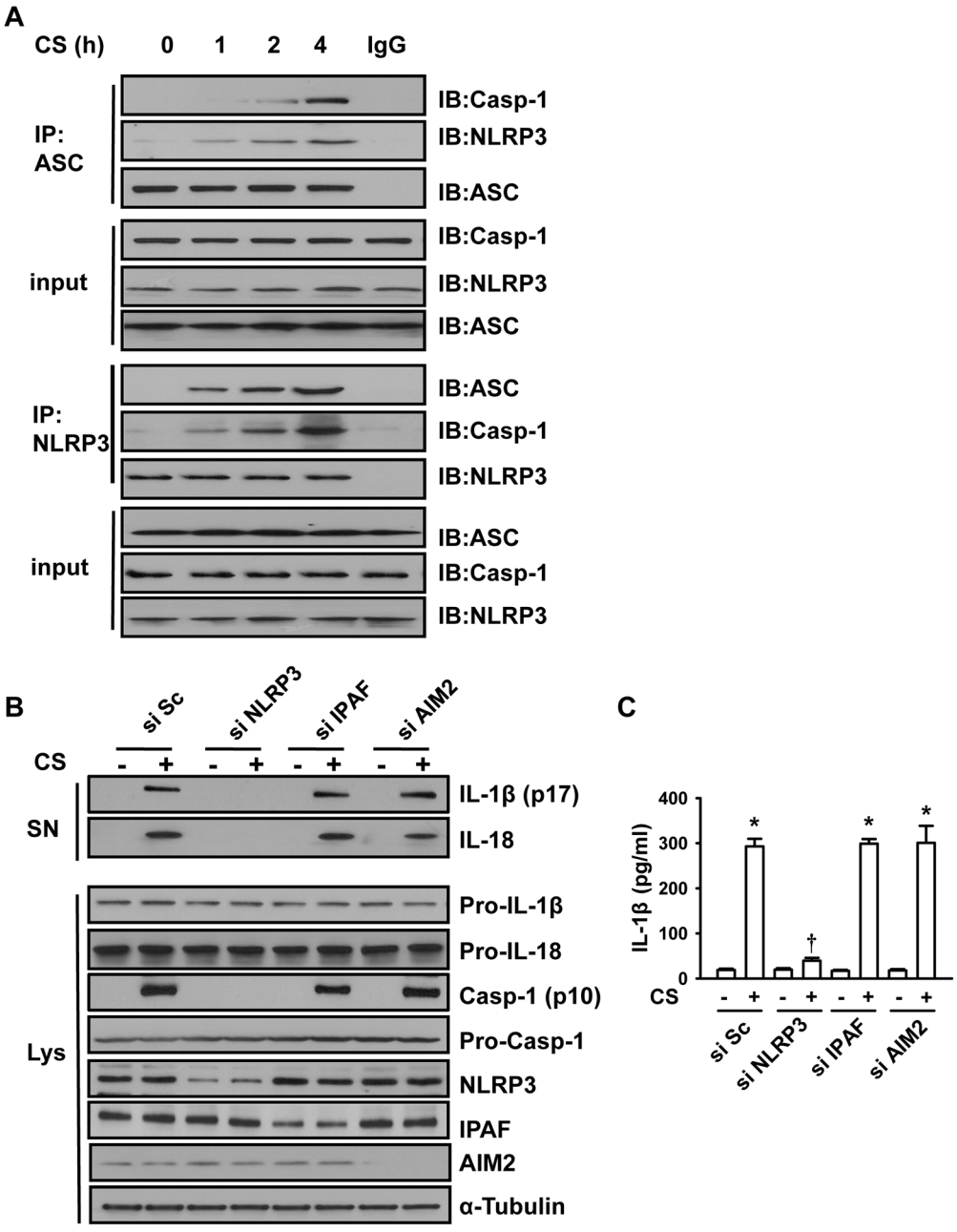

FIGURE 3. Cyclic stretch stimulates IL-1β production via NLRP3-dependent signaling pathway

A. Cyclic stretch (CS) induced NLRP3 inflammasome activation in AMs. AMs were exposed to 20% cyclic stretch for the indicated time. The assembly of NLRP3 inflammasome was detected using immunoprecipitation with anti-ASC Ab followed by immunoblotting for NLRP3, ASC, and caspase-1 cleavage product p10 fragments (Casp-1). The NLRP3 activation was confirmed by using immunoprecipitation with anti-NLRP3 Ab followed by immunoblotting for ASC, NLRP3, and Casp-1. ***B***. Effects of depletion of NLRP3, IPAF, or AIM2 with respective siRNAs on IL-1β, IL-18 and mature Casp-1 production following 20% cyclic stretch for 4 h. IL-1β and IL-18 release in the culture supernatants (SN) of AMs and levels of Pro-IL-1β, Pro-IL-18, Pro-Casp-1 and Casp-1 in cell lysate (Lys) were determined by Western blot analysis. A scrambled siRNA (si Sc) was

used as a negative control. ***C***. The levels of IL-1β in cell-culture media were measured by ELISA. The graph shows the mean and SEM from 3 independent experiments. *$p < 0.05$ vs. the control (static) group. † $p < 0.05$ vs. si Sc+CS group.

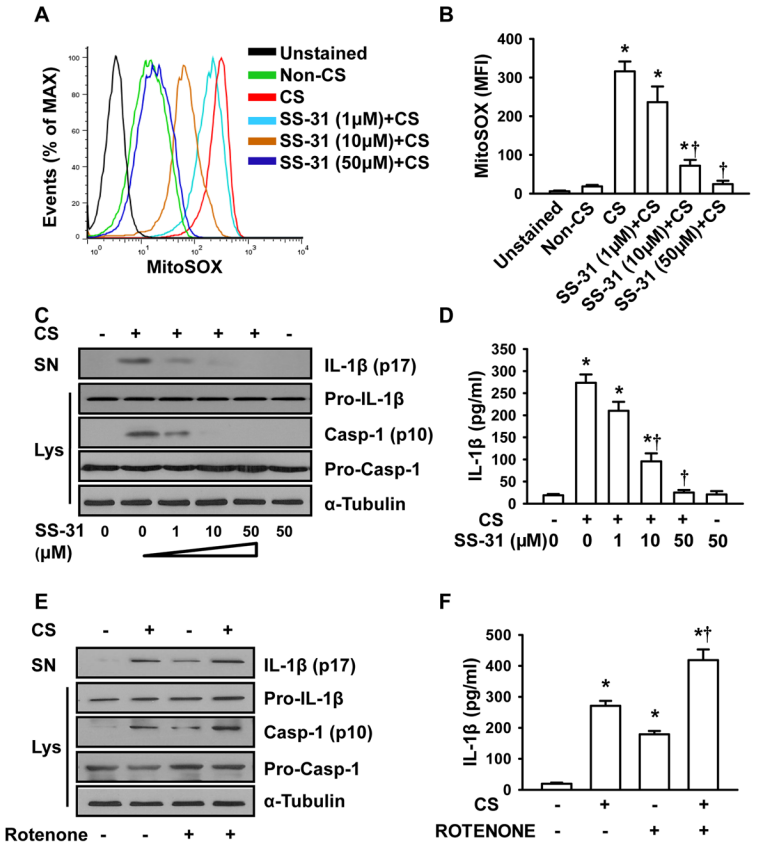

FIGURE 4. Mitochondrial ROS are required for NLRP3 inflammasome activation following cyclic stretch

A. Representative histograms of flow cytometry experiments demonstrating the effects of cyclic stretch and SS-31 on mitochondrial ROS generation. AMs were pretreated with SS-31 peptide (10 μM) for 24 h prior to stretch. AMs were stained with MitoSOX for 30 min and analyzed by flow cytometry. ***B***. Quantitative data showing changes in mean fluorescent intensity (MFI) of MitoSOX following stretch and SS-31 treatment (n=3). ***C***. SS-31 dose-dependently inhibited IL-1β release and caspase-1 activation following 20% cyclic stretch for 4 h. IL-1β release in the culture supernatants (SN) of AMs and levels of Pro-IL-1β, Pro-Casp-1 and Casp-1 in cell lysate (Lys) were determined by Western blot analysis. ***D***. IL-1β in cell-culture media was measured by ELISA (n=3). ***E***. Effects of rotenone on IL-1β release and caspase-1 activation following 20% cyclic stretch for 4 h. ***F***. IL-1β in cell-culture media was measured by ELISA (n=3). *$p < 0.05$ vs. the control (static) group. † $p < 0.05$ vs. CS alone group.

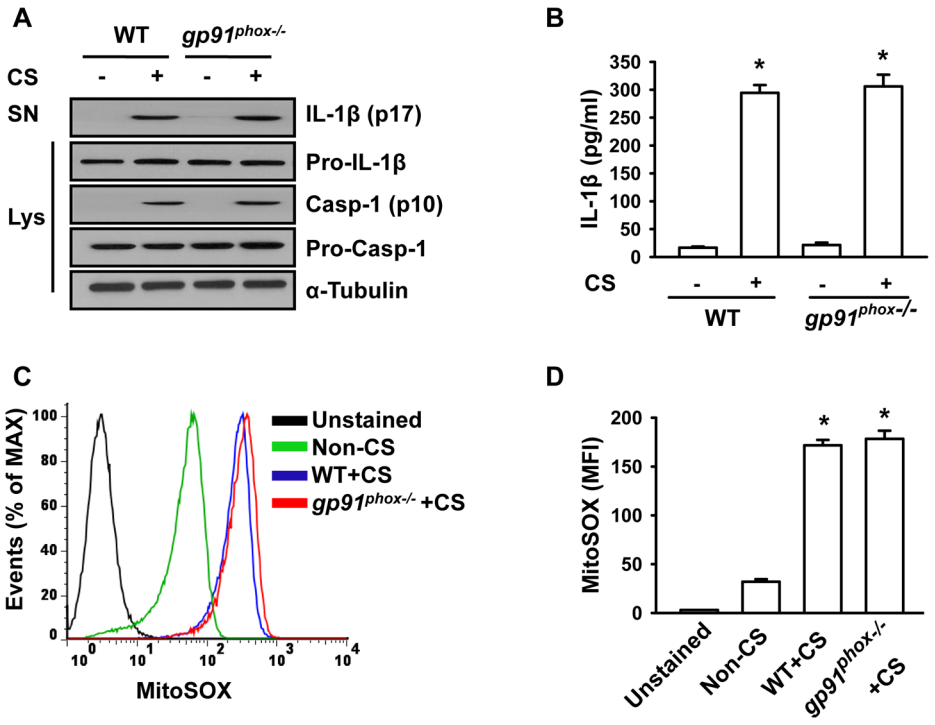

FIGURE 5. NADPH oxidase-derived ROS do not contribute to cyclic stretch-induced NLRP3 inflammasome activation

A. AMs isolated from *gp91*$^{phox-/-}$mice show no change in IL-1β release following stretch. Wild type and *gp91*$^{phox-/-}$AMs were subjected to 20% cyclic stretch for 4 h. IL-1β release in the culture supernatants (SN) of AMs and levels of Pro-IL-1β, Pro-Casp-1 and Casp-1 in cell lysate (Lys) were determined by Western blot analysis. ***B***. The levels of IL-1β in cell-culture media were measured by ELISA (n=3). ***C***. Representative histograms of flow cytometry experiments demonstrating the effects of cyclic stretch on mitochondrial ROS generation in *gp91*$^{phox-/-}$ and wild type AMs. ***D***. Quantitative data showing changes in mean fluorescent intensity (MFI) of MitoSOX following stretch (n=3). *$p < 0.05$ vs. the control (static) group.

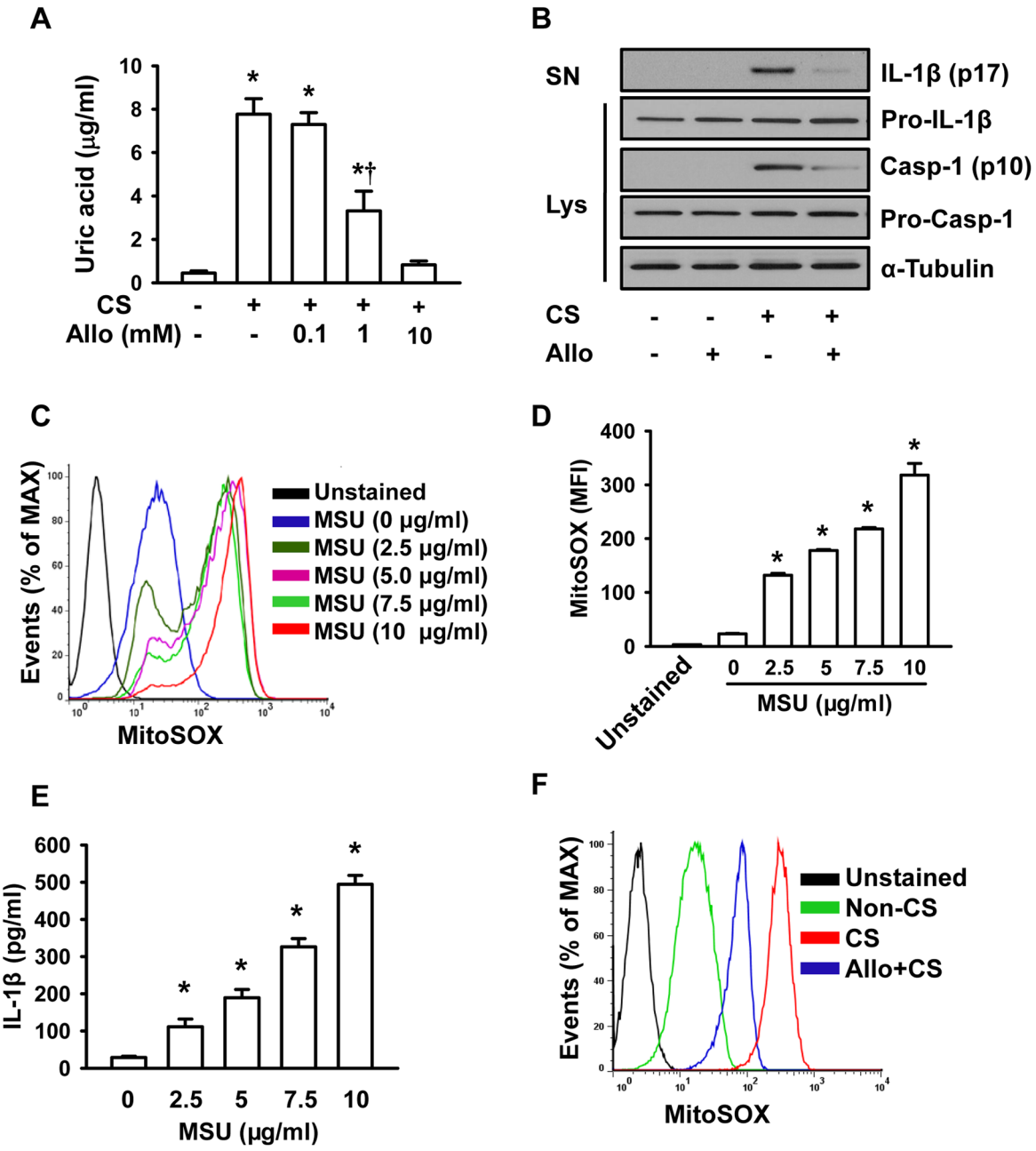

FIGURE 6. Uric acid production by cyclic stretch contributes to NLRP3 inflammasome activation partially through mitochondrial ROS

A. Effects of cyclic stretch and allopurinol on uric acid production. AMs were exposed to 20% cyclic stretch for 4 h in the absence and presence of allopurinol pretreatment for 4 h. Uric acid concentrations were measured in the media of cultured AMs post stretch as described in *Materials and Methods*. ***B***. Effects of allopurinol on IL-1β release and caspase-1 activation. AMs were subjected to 20% cyclic stretch for 4 h. IL-1β release in the culture supernatants (SN) of AMs and levels of Pro-IL-1β, Pro-Casp-1 and Casp-1 in cell lysate (Lys) were determined by Western blot analysis. ***C***. Representative histograms of flow cytometry experiments demonstrating the effects of MSU on mitochondrial ROS

generation. ***D***. Quantitative data showing the effects of MSU on mean fluorescent intensity (MFI) of MitoSOX (n=3). ***E***. Effects of MSU on IL-1β release measured by ELISA (n=3). ***F***. Representative histograms of flow cytometry experiments demonstrating the effects of allopurinol on cyclic stretch-induced mitochondrial ROS generation. *$p < 0.05$ vs. the control (static, *A*) or non-MSU treated (*D*, *E*) group. † $p < 0.05$ vs. CS alone group.

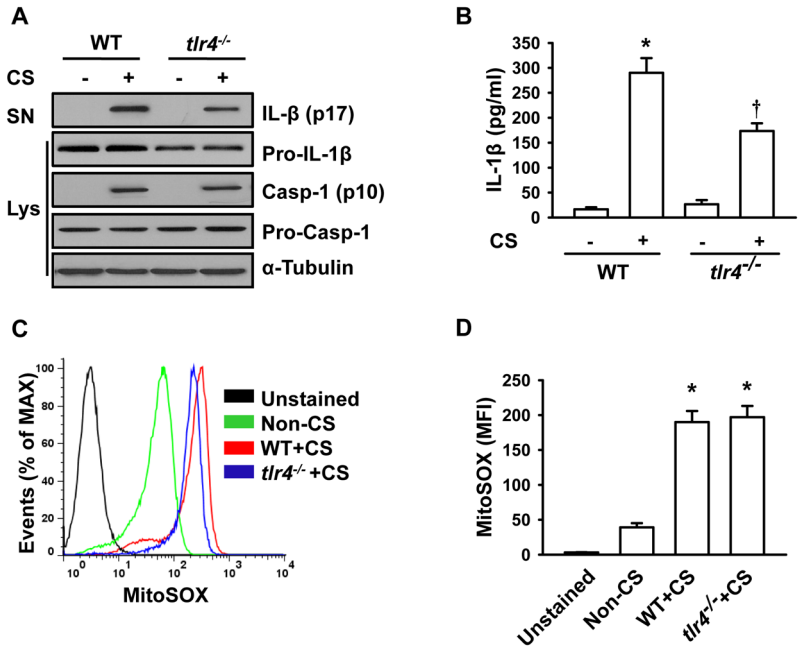

FIGURE 7. IL-1β production following cyclic stretch occurs via TLR4 signaling. ***A*** AMs isolated from *tlr4*$^{-/-}$ mice show less IL-1β release following stretch. Wild type and *tlr4*$^{-/-}$ AMs were subjected to 20% cyclic stretch for 4 h. IL-1β release in the culture supernatants (SN) of AMs and levels of Pro-IL-1β, Pro-Casp-1 and Casp-1 in cell lysate (Lys) were determined by Western blot analysis. ***B***. The levels of IL-1β in cell-culture media were measured by ELISA (n=3). ***C***. Representative histograms of flow cytometry experiments demonstrating the effects of cyclic stretch on mitochondrial ROS generation in *tlr4*$^{-/-}$ and wild type AMs. ***D***. Quantitative data showing changes in mean fluorescent intensity (MFI) of MitoSOX following stretch (n=3). *$p < 0.05$ vs. the control (static) group. † $p < 0.05$ vs. WT+CS group.

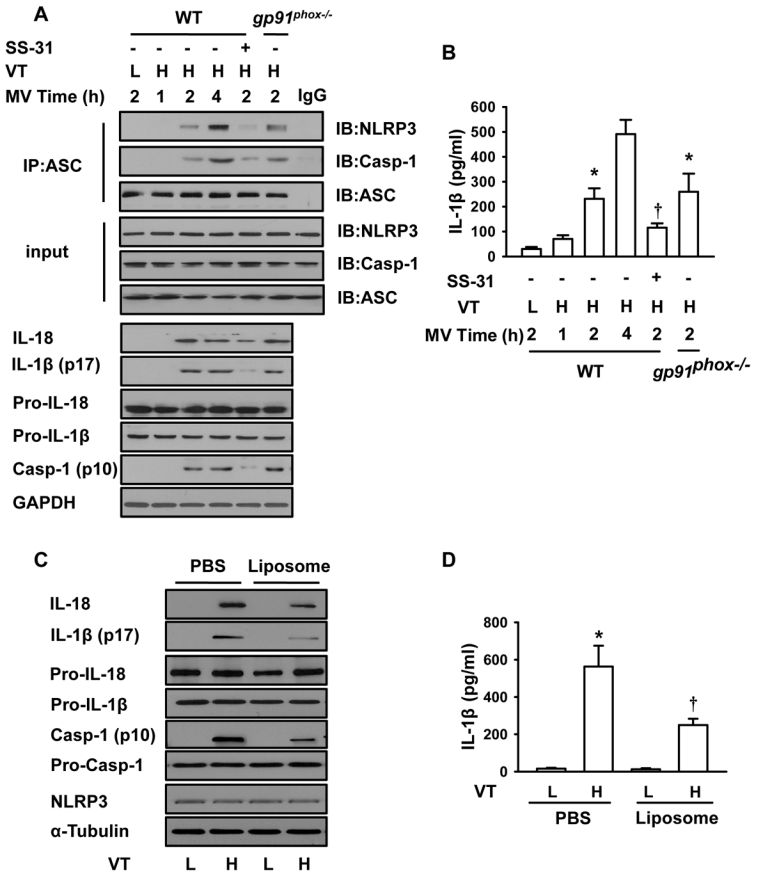

FIGURE 8. Mechanical ventilation with a high tidal volume activates NLRP3 inflammasome in mouse lungs

Wild type and *gp91*$^{phox-/-}$ mice were ventilated with a normal (L) or high (H) tidal volume for the indicated times. At the end of experiments, lung tissue and BAL fluid were recovered. ***A***. Effects of mechanical ventilation and SS-31 on NLRP3 inflammasome activation and subsequent release of IL-1β and IL-18. Top: The assembly of NLRP3 inflammasome was detected using immunoprecipitation with anti-ASC Ab followed by immunoblotting for NLRP3, ASC, and caspase-1 cleavage product p10 fragments (Casp-1). Bottom: The levels of mature IL-1β, mature IL-18, Pro-IL-1β, Pro-IL-18, Pro-Casp-1 and Casp-1 in lung homogenates were determined by Western blot analysis. ***B***. The levels of IL-1β in BAL fluid were measured by ELISA. The graph shows the mean and SEM from six mice. ***C***. Effects of depletion of AMs with liposome on mechanical ventilation-induced release of IL-1β and IL-18, and caspase-1 activation. The levels of mature IL-1β, mature IL-18, Pro-IL-1β, Pro-IL-18, Pro-Casp-1 and Casp-1 in lung homogenates were determined by Western blot analysis. ***D***. The levels of IL-1β in BAL fluid were measured by ELISA (n=6). *$p < 0.05$ vs. the control group (L). † $p < 0.05$ vs. WT+H group (*B*, 2h alone) or PBS +H group (*D*).

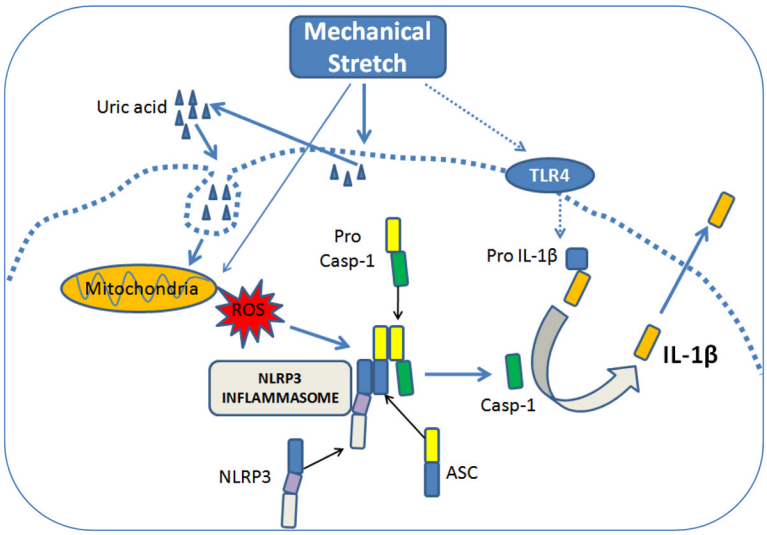

FIGURE 9. Model of inflammasome activation by mechanical stretch

ASC, apoptosis-associated speck-like protein containing a CARD domain; Casp-1, caspase-1; NLRP3, NOD-like receptor containing pyrin domain 3; ROS, reactive oxygen species.